Wireless Power Transfer System With High-Order Compensation Network Based on Parity-Time-Symmetric Principle and Relay Coil

Yuhu Qu, Bo Zhang, *Senior Member, IEEE*, Wenchao Gu, and Xujian Shu

***Abstract*—The parity-time (PT) symmetric principle has been proved that it can improve the degree of freedom of the wireless power transfer (WPT) system with multiple repeaters, while maintaining constant transfer efficiency and transmission power. This article presents a novel three-coil WPT system with S/S/PS compensation network based on the PT symmetry principle to further expand the exact PT-symmetric region and increase the output power. First, the PS compensation network increases the order of the system. This problem has been solved by simplifying the PS compensation network to the S compensation network with equivalent circuit theory. Second, it is found that the proposed system has smaller critical coupling coefficient and is able to provide higher output power compared to traditional three-coil PT-symmetric system. Third, the capacitance distribution ratio can be designed to make the system adapt to different application scenarios. Finally, an experimental prototype 48 W is developed to verify the proposed system.**

***Index Terms*—Equivalent circuit method, parity-time (PT) symmetry, relay coil, wireless power transfer (WPT).**

I. Introduction

WIRELESS power transfer (WPT) technology without any physical connection has the characteristics of high flexibility, convenience, and safety. It has attracted increasing attention of researchers and has been widely applied to various applications such as electric vehicles [1], [2], biomedical implants [3], and portable electronics [4].

Being a research hotspot in recent years, the system of magnetic coupling resonance WPT technology has an obvious drawback: the low degree of freedom. The transfer efficiency and output power decrease significantly with the increase of transmission distance [5], which highly limits the development and application of WPT technology [6].

Manuscript received 8 February 2022; revised 25 May 2022 and 22 July 2022; accepted 20 August 2022. Date of publication 25 August 2022; date of current version 10 October 2022. This work was supported by the Key Program of the National Natural Science Foundation of China under Grant 52130705. Recommended for publication by Associate Editor A. Kuperman. *(Corresponding author: Bo Zhang.)*

Yuhu Qu, Bo Zhang, and Wenchao Gu are with the School of Electric Power, South China University of Technology, Guangzhou 510640, China (e-mail: qyh2761@163.com; epbzhang@scut.edu.cn; epguwenchao@mail.scut.edu.cn).

Xujian Shu is with the College of Electrical Engineering and Automation, Fuzhou University, Fuzhou 350000, China (e-mail: epshuxujian@163.com).

Color versions of one or more figures in this article are available at https://doi.org/10.1109/TPEL.2022.3201693.

Digital Object Identifier 10.1109/TPEL.2022.3201693

The design of the WPT system generally follows two principles: maximum energy efficiency principle and maximum power transfer (MPT) principle [7]. The transfer efficiency will be less than 50% when the WPT system follows MPT principle. Hence, the WPT system needs to meet the output power firstly and then maintain the maximum efficiency by varying coupling coefficient. A variety of methods have been proposed in recent years to maintain constant output power and higher transfer efficiency: frequency tracking [8], [9], [10], impedance transformation networks [11], [12], [13], load impedance matching [14], [15], and uniform magnetic field by configuration coils [16]. Most of them require complex control algorithms and additional circuits, which will increase the complexity of the WPT system. Therefore, it is necessary to explore new WPT mechanisms.

In traditional quantum mechanics, the Hamiltonian must be represented by the Hermitian operator, which is to ensure that the eigenvalues of the Hamiltonian of the quantum system are real numbers, and that the time evolution of the quantum system is unitary. However, the Hamiltonian of the Hermitian operator is only a sufficient but nonessential condition for observability.

Bender and Boettcher [17] first proposed that a series of non-Hermitian Hamiltonians based on parity-time (PT) symmetry also has real energy eigenvalues within a certain range of parameters. The role of the parity operator $\hat{P}$ is space inversion, i.e., the momentum operator $\hat{p} \rightarrow -\hat{p}$ and the position operator $\hat{x} \rightarrow -\hat{x}$; the role of the time reversal operator $\hat{T}$ is to make the momentum operator $\hat{p} \rightarrow -\hat{p}$, the position operator $\hat{x} \rightarrow -\hat{x}$, and the imaginary unit $\hat{i} \rightarrow -\hat{i}$. A PT-symmetric system means that the system characteristics are invariant under the combined operation of $\hat{P}$ and $\hat{T}$ operators. In optical systems, quantum systems described by non-Hermitian PT-symmetric Hamiltonians can be realized through gain-loss balance, so PT symmetry has been intensively studied in the field of optics [18], [19]. Later, the concept of PT symmetry was gradually used to describe systems with gain and loss.

In 2017, researchers of Stanford University first applied the PT symmetry principle to WPT technology, enabling the receiving coil to maintain constant power at any position within 1 m [20]. The negative resistance is constructed by an operational amplifier, which is the gain part. A bulb acts as a load to form the loss part in the receiver. In the exact PT-symmetric region, the system achieves gain and loss balance. Hence, the WPT system can maintain constant transfer efficiency and output

power regardless of the change of coupling coefficient. The disadvantage of the proposed system is that the power level is too low to be applied in practice. Since this method can easily overcome the difficulties of the traditional resonant WPT system without adding additional circuits and complex control methods, the WPT systems based on PT symmetry have attracted great interest from researchers.

To improve the output power level of the PT-symmetric system, Zhou et al. [21] used a self-oscillating controlled half-bridge inverter to provide nonlinear saturable gain. This method was applied to the drone-in-flight wireless charging system with approximately constant output power of 10 W and constant transfer efficiency of 93.6%. Watt-level PT-symmetric WPT system can be realized by this method. Subsequently, the PT-symmetric system was applied to electric vehicle charging with multiple decoupled receiving coils [22], which expands the application scenarios of PT symmetry.

The relay coil has been proven that it can extend the transmission distance and improve the transfer efficiency of the WPT system significantly [23], [24]. A WPT system with multiple relay coils based on the concept of PT symmetry was proposed by Shu et al. [25], which can maintain constant output power and transfer efficiency at different transmission distances. The difference between an odd and even number of relay coils was also analyzed. At the same time, the proposed method can reduce the critical coupling coefficient and improve the flexibility of the WPT system.

When the parameters of the PT-symmetric system are fixed, the receiving coil is only moved in the fixed exact PT-symmetric region to maintain constant transmission efficiency and output power. In order to further extend the transmission distance, a novel WPT system with the S/S/PS compensation network based on the PT-symmetric principle is proposed in this article. The PS compensation network of the receiving coil increases the complexity of the system model. First, the high-order compensation network is converted to the low-order compensation network by the equivalent circuit method. Subsequently, the mathematical model of the system is established by the coupling mode theory (CMT). Then, the analytical expressions of operating frequency, output power and transmission efficiency are obtained. And the characteristics of the proposed system are analyzed. The main works and contributions are as follows.

1) The equivalent circuit method is used to simplify the PS compensation network to the S compensation network, which makes the system easy to be modeled by CMT.
2) The equivalent load resistance of the proposed system is greatly reduced by using the PS compensation network. Then, the critical coupling coefficient k_c is effectively reduced. Therefore, the proposed system significantly expands the exact PT-symmetric region.
3) The sum of the parallel and series capacitances is equal to the series capacitance of the original PT-symmetric system, which is convenient for designing and modifying the system parameters.
4) The PS compensation network can also be a tradeoff between transfer efficiency and transmission distance by adjusting the capacitance distribution ratio in different practical application scenarios.

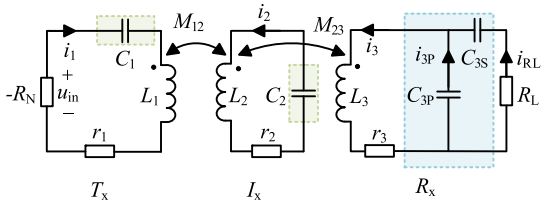

Fig. 1. Schematic of the S/S/PS three-coil WPT system based on PT-symmetric principle.

The rest of this article is organized as follows. In Section II, the PS compensation network is converted into the S compensation network by the equivalent circuit method, then, the CMT is used to model and analyze the proposed system. The system is designed in Section III. A 48 W experimental prototype is constructed in Section IV to validate the proposed theoretical analysis and system design method. Finally, Section V concludes this article.

II. Theoretical Analysis of the S/S/PS Type Three-Coil WPT System

A. Equivalent Circuit Model

The proposed three-coil WPT system with S/S/PS compensation network based on the PT-symmetric principle is shown in Fig. 1. $-R_N$ is a negative resistance that is used as a power source to provide input voltage u_{in} to the system. L_1, L_2, and L_3 are the inductances of the transmitting coil, relay coil, and receiving coil, respectively. r_1, r_2, and r_3 are the internal resistances of coils. M_{12} and M_{23} are the mutual inductances between adjacent coils. M_{13} is the mutual inductance between nonadjacent coils. For a WPT system with relay coils, the magnetic field coupling between nonadjacent coils can be ignored due to the large separation between L_1 and L_3, so M_{13} can be neglected in theoretical analysis. The rationality of this assumption will be demonstrated in Section III-B. C_1 and C_2 are the tuning capacitors of the transmitting coil and rely coil, respectively. C_{3P} and C_{3S} are the tuning capacitors of the receiving coil. R_L is the load resistance.

The WPT system can be modeled by CT and CMT. The WPT system with relay coil is a high-order system and the parallel capacitor will also increase the order of the system model, which makes CT model difficult to obtain analytical solutions to analyze the transmission characteristics [11]. Compared with CT, CMT simplifies the analysis by reducing the order of the differential equations by half [27]. Therefore, the proposed WPT system will be analyzed by CMT in this article.

To the best of authors' knowledge, CMT is used to analyze the WPT system with the compensation network composed of a passive component at present. For the WPT system with the high-order compensation network, there is no general method to obtain coupled differential equations. In order to establish the coupled-mode equations, the PS compensation network is simplified to the S compensation network by the equivalent circuit

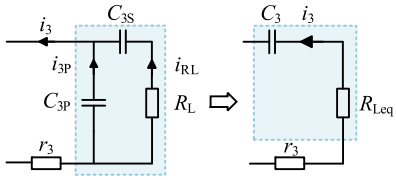

Fig. 2. Equivalent transformation of the PS compensation network.

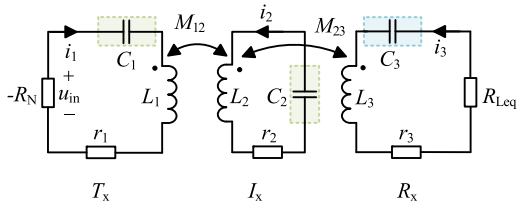

Fig. 3. Equivalent circuit of the S/S/PS three-coil WPT system.

method, as shown in Fig. 2. The equivalent circuit parameters can be derived as

$$\begin{cases} C_3 = \frac{(C_{3S}+C_{3P})^2+\omega^2 C_{3S}^2 C_{3P}^2 R_L^2}{C_{3S}+C_{3P}+\omega^2 C_{3S}^2 C_{3P} R_L^2} \\ R_{Leq} = \frac{C_{3S}^2 R_L}{(C_{3S}+C_{3P})^2+\omega^2 C_{3S}^2 C_{3P}^2 R_L^2}. \end{cases} \tag{1}$$

It can be seen from (1) that $\omega^2 {C_{3S}}^2 {C_{3P}}^2 {R_L}^2 << (C_{3S}+C_{3P})^2$ and $\omega^2 {C_{3S}}^2 C_{3P} {R_L}^2 << C_{3S}+C_{3P}$, hence (1) can be simplified as

$$\begin{cases} C_3 = C_{3S} + C_{3P} \\ R_{Leq} = \frac{C_{3S}^2 R_L}{(C_{3S}+C_{3P})^2} \end{cases}. \tag{2}$$

In order to simplify the equation and facilitate the system characteristic analysis, we define α ($0<\alpha<1$) as the capacitance distribution ratio

$$\begin{cases} C_{3S} = \alpha C_3 \\ C_{3P} = (1-\alpha) C_3 \end{cases}. \tag{3}$$

Therefore, the equivalent load resistance can be expressed as

$$R_{Leq} = \alpha^2 R_L. \tag{4}$$

B. Coupled Modeling

Fig. 3 shows the equivalent circuit of the proposed system. Considering that the relay coil is only used to extend the transmission, its internal resistance r_2 can be ignored. According to Fig. 3, the coupled-mode equations of the equivalent system can be written as

$$\frac{\mathrm{d}}{\mathrm{d}t}\begin{bmatrix} \mathbf{a}_1 \\ \mathbf{a}_2 \\ \mathbf{a}_3 \end{bmatrix} = \begin{bmatrix} \mathrm{j}\omega_1 + g - \gamma_1 & -\mathrm{j}\kappa_{12} & 0 \\ -\mathrm{j}\kappa_{12} & \mathrm{j}\omega_2 & -\mathrm{j}\kappa_{23} \\ 0 & -\mathrm{j}\kappa_{23} & \mathrm{j}\omega_3 - \gamma_3 - \gamma_{Leq} \end{bmatrix} \times \begin{bmatrix} \mathbf{a}_1 \\ \mathbf{a}_2 \\ \mathbf{a}_3 \end{bmatrix} \tag{5}$$

where $\boldsymbol{a}_n = \sqrt{L_n}\,(i_n \pm j\omega_n C_n u_{Cn})/2$, (n = 12,3) are the coupled modes, and $|a_n|^2$ are corresponding to the energy stored in resonators. $\omega_n = 1/\sqrt{L_n C_n}$ are the natural resonant frequencies of resonators. $\gamma_n = r_n/(2L_n)$ are the intrinsic loss rate of resonators, $\gamma_{Leq} = R_{Leq}/(2L_3)$ is the loss rate of the equivalent load. $g = 2\ V_{dc}/(\pi\sqrt{2L_1}|\boldsymbol{a}_1|)$ is the gain rate of the transmitter T_X. $\kappa_{mn} = \omega_0 M_{mn}/(2\sqrt{L_m L_n})$(m = 12,3; m≠n) are the coupling coefficients between two adjacent coils. The power transfer efficiency of the system reaches the maximum when the relay coil I_X is located between T_X and R_X, hence, the coupling coefficient between the coils can be set as $\kappa_{12} = \kappa_{23} = \kappa$.

To get the operating frequencies, it is assumed that the steady solutions are the form $[\boldsymbol{a}_1, \boldsymbol{a}_2, \boldsymbol{a}_3]^T = [A_1, A_2, A_3]^T \mathrm{e}^{\mathrm{j}\omega t}$, where A_n are the amplitudes of $\boldsymbol{a}_n$. And three resonators maintain the same natural resonant frequency, that is $\omega_1 = \omega_2 = \omega_3 = \omega_0$. According to (5), the frequency characteristic equation of the system is given (6) shown at the bottom of this page

The imaginary and real parts of (6) can be separated as

$$\begin{cases} (\omega-\omega_0)\left[2\kappa^2 - (\omega-\omega_0)^2 + (\gamma_1 - g)(\gamma_3+\gamma_{Leq})\right] = 0 \\ (\gamma_1 - g + \gamma_3 + \gamma_{Leq})\left[\kappa^2 - (\omega-\omega_0)^2\right] = 0. \end{cases} \tag{7}$$

The steady solutions with real ω can be derived according to (7). When the coupling coefficient of the system is arbitrary, and $\omega = \omega_0$ is always the solution of the equations. At this time, the system is in the resonant state, and the operating frequency is equal to the natural resonant frequency of the system. Then, the gain coefficient g can be deduced as

$$g = \gamma_1 + \gamma_3 + \gamma_{Leq}. \tag{8}$$

Substituting (8) into (5), the amplitude of the modes $\boldsymbol{a}_1$ and $\boldsymbol{a}_3$ can be derived as

$$|\boldsymbol{a}_1| = |\boldsymbol{a}_3| = \frac{U_{in}}{2\sqrt{L_1}\,(\gamma_1 + \gamma_3 + \gamma_{Leq})}. \tag{9}$$

Then, the output power and transfer efficiency of the system can be expressed as

$$P_{out} = 2\gamma_{Leq}|\boldsymbol{a}_3|^2 = \frac{\gamma_{Leq} U_{in}^2}{2L_1(\gamma_1 + \gamma_3 + \gamma_{Leq})^2} \tag{10}$$

$$\begin{vmatrix} \mathrm{j}(\omega-\omega_0) - g + \gamma_1 & \mathrm{j}\kappa & 0 \\ \mathrm{j}\kappa & \mathrm{j}(\omega-\omega_0) & \mathrm{j}\kappa \\ 0 & \mathrm{j}\kappa & \mathrm{j}(\omega-\omega_0) + \gamma_3 + \gamma_{Leq} \end{vmatrix} = 0. \tag{6}$$

$$\eta = \frac{2\gamma_{\mathrm{Leq}}|\boldsymbol{a}_3|^2}{2\gamma_1|\boldsymbol{a}_1|^2 + 2\gamma_3|\boldsymbol{a}_3|^2 + 2\gamma_{\mathrm{Leq}}|\boldsymbol{a}_3|^2} = \frac{\gamma_{\mathrm{Leq}}}{\gamma_1 + \gamma_3 + \gamma_{\mathrm{Leq}}}. \tag{11}$$

It can be seen from (10) and (11) that the output power and transfer efficiency of the proposed system are independent of the coupling coefficient κ, and only relate to the parameters of the system as well as the loss rate of the equivalent load.

When $\omega \neq \omega_0$ and the steady operating frequencies ω can be derived according to (7), there is a critical coupling coefficient κ_{C} that divides the operation region into two cases: exact PT-symmetric region and broken PT-symmetric region

$$\kappa_c = \frac{\sqrt{2}\,(\gamma_3 + \gamma_{\mathrm{Leq}})}{\omega_0}. \tag{12}$$

From (12), the critical coupling coefficient κ_{C} only depends on the intrinsic loss rate of the oscillator R_{X} and the loss rate of the equivalent load. As can be seen from (4) that the equivalent load resistance R_{Leq} of the proposed system is smaller than the actual load resistance R_{L}. Substituting (4) into (12), when the load resistance R_{L} of the three-coil WPT system is constant, the critical coupling coefficient κ_{C} of the S/S/PS system is much smaller than that of the S/S/S system. Therefore, the S/S/PS compensation network can expand the exact PT-symmetric area of the three-coil PT-symmetric system.

1) Exact PT-Symmetric Region ($\kappa > \kappa_C$): In this case, the gain coefficient g and operating frequency ω can be derived as

$$\begin{cases} g = \gamma_1 + \gamma_3 + \gamma_{\mathrm{Leq}} \\ \omega = \omega_0 \pm \sqrt{2\kappa^2 - (\gamma_3 + \gamma_{\mathrm{Leq}})^2}. \end{cases} \tag{13}$$

The amplitude of the mode can be deduced by (5) and (13)

$$|\boldsymbol{a}_1| = |\boldsymbol{a}_3| = \frac{U_{\mathrm{in}}}{2\sqrt{L_1}\,(\gamma_1 + \gamma_3 + \gamma_{\mathrm{Leq}})}. \tag{14}$$

Then, the output power P_{out} and transfer efficiency η of the system can be described as

$$P_{\mathrm{out}} = 2\gamma_{\mathrm{Leq}}|\boldsymbol{a}_3|^2 = \frac{\gamma_{\mathrm{Leq}}U_{\mathrm{in}}^2}{2L_1(\gamma_1 + \gamma_3 + \gamma_{\mathrm{Leq}})^2} \tag{15}$$

$$\eta = \frac{2\gamma_{\mathrm{Leq}}|\boldsymbol{a}_3|^2}{2\gamma_1|\boldsymbol{a}_1|^2 + 2\gamma_3|\boldsymbol{a}_3|^2 + 2\gamma_{\mathrm{Leq}}|\boldsymbol{a}_3|^2} = \frac{\gamma_{\mathrm{Leq}}}{\gamma_1 + \gamma_3 + \gamma_{\mathrm{Leq}}}. \tag{16}$$

It can be seen from (10), (11), (15), and (16) that the expressions of output power P_{out} and transfer efficiency η are consistent with those obtained in the resonance state, so the output power and transfer efficiency are independent of the coupling coefficient, i.e., in the exact PT-symmetric region, the output power and transfer efficiency remain constant when the distance between the transmission coil, relay coil, and receiving coil changes equidistantly.

The proposed system supports three stable operating frequencies when the system is in the exact PT-symmetric region, which means that the system oscillates at three frequencies automatically, and the operating frequency varies with the coupling coefficient due to the nonlinear saturation gain.

TABLE I
COMPARISON BETWEEN THE PERFORMANCE OF THE PROPOSED SYSTEM AND THE S/S/S TYPE PT-SYMMETRIC SYSTEM

	S/S/PS	S/S/S
Critical coupling coefficient	$\frac{r_3 + \alpha^2 R_{\mathrm{L}}}{\sqrt{2}\omega_0 L_3}$	$\frac{r_3 + R_{\mathrm{L}}}{\sqrt{2}\omega_0 L_3}$
Output power	$\frac{\alpha^2 R_{\mathrm{L}} U_{\mathrm{in}}^2 L_1 L_3}{\left(r_1 L_3 + r_3 L_1 + \alpha^2 R_{\mathrm{L}} L_1\right)^2}$	$\frac{R_{\mathrm{L}} U_{\mathrm{in}}^2 L_1 L_3}{\left(r_1 L_3 + r_3 L_1 + R_{\mathrm{L}} L_1\right)^2}$
Transfer efficiency	$\frac{\alpha^2 R_{\mathrm{L}} L_1}{r_1 L_3 + r_3 L_1 + \alpha^2 R_{\mathrm{L}} L_1}$	$\frac{R_{\mathrm{L}} L_1}{r_1 L_3 + r_3 L_1 + R_{\mathrm{L}} L_1}$

2) Broken PT-Symmetric Region ($0 < \kappa < \kappa_C$): In this case, the PT symmetry is broken, the gain coefficient g and operating frequency ω can be derived as

$$\begin{cases} g = \gamma_1 + \frac{\kappa^2}{\gamma_3 + \gamma_{\mathrm{Leq}}} \\ \omega = \omega_0 \pm \kappa \end{cases}. \tag{17}$$

By substituting (17) into (5), the amplitude of the modes $\boldsymbol{a}_1$ and $\boldsymbol{a}_3$ can be given as

$$|\boldsymbol{a}_1| = \frac{(\gamma_3 + \gamma_{\mathrm{Leq}})\,U_{\mathrm{in}}}{2\sqrt{L_1}\,(\gamma_1\gamma_3 + \gamma_1\gamma_{\mathrm{Leq}} + \kappa^2)} \tag{18}$$

$$|\boldsymbol{a}_3| = \frac{\kappa}{\gamma_3 + \gamma_{\mathrm{Leq}}}\,|\boldsymbol{a}_1| = \frac{\kappa V_{\mathrm{in}}}{2\sqrt{L_1}\,(\gamma_1\gamma_3 + \gamma_1\gamma_{\mathrm{Leq}} + \kappa^2)}. \tag{19}$$

The output power P_{out} and transfer efficiency η of the system can be obtained as

$$P_{\mathrm{out}} = 2\gamma_{\mathrm{Leq}}|\boldsymbol{a}_3|^2 = \frac{\gamma_{\mathrm{Leq}}\kappa^2 U_{\mathrm{in}}^2}{2L_1(\gamma_1\gamma_3 + \gamma_1\gamma_{\mathrm{Leq}} + \kappa^2)^2} \tag{20}$$

$$\eta = \frac{2\gamma_{\mathrm{Leq}}|\boldsymbol{a}_3|^2}{2\gamma_1|\boldsymbol{a}_1|^2 + 2\gamma_3|\boldsymbol{a}_3|^2 + 2\gamma_{\mathrm{Leq}}|\boldsymbol{a}_3|^2} = \frac{\gamma_{\mathrm{Leq}}\kappa^2}{\gamma_1(\gamma_3 + \gamma_{\mathrm{Leq}})^2 + \kappa^2\,(\gamma_3 + \gamma_{\mathrm{Leq}})}. \tag{21}$$

From (20) and (21), it is obvious that the expressions of output power P_{out} and transfer efficiency η are related to the coupling coefficient κ. In the broken PT-symmetric region, the output power and transfer efficiency vary with the transmission distance. Therefore, the WPT system should be avoided to operate in the broken PT-symmetric region to ensure the stable operation of the system.

C. Transmission Characteristics

The comparison between the proposed system and the S/S/S PT-symmetric system is listed in Table I. The characteristic expressions of CMT are reorganized into the expressions of CT to make the comparison more intuitive. Then, the corresponding transmission characteristic curves can be obtained according to the system characteristic expressions in Table I.

It can be manifest that the transfer efficiency and the critical coupling coefficient are only related to the load resistance and

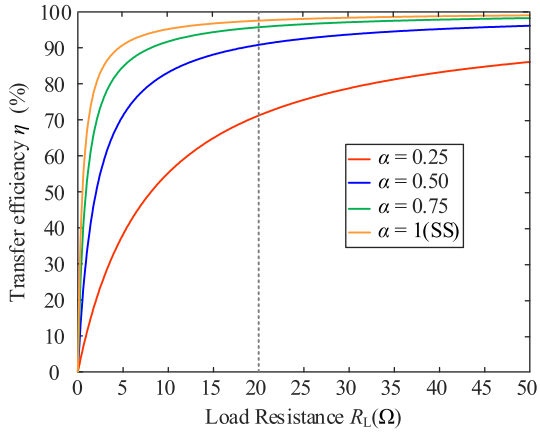

Fig. 4. Curves of transfer efficiency versus load resistance with different capacitance distribution ratios.

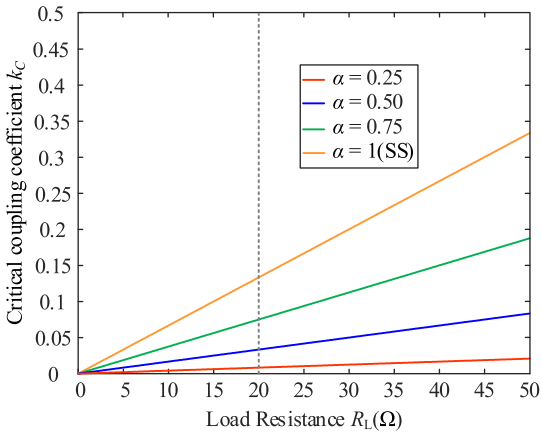

Fig. 5. Curves of critical coupling coefficient versus load resistance with different capacitance distribution ratios.

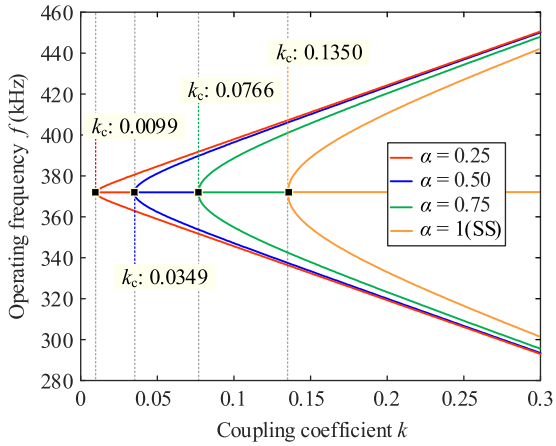

Fig. 6. Frequency bifurcation in the exact PT-symmetric region.

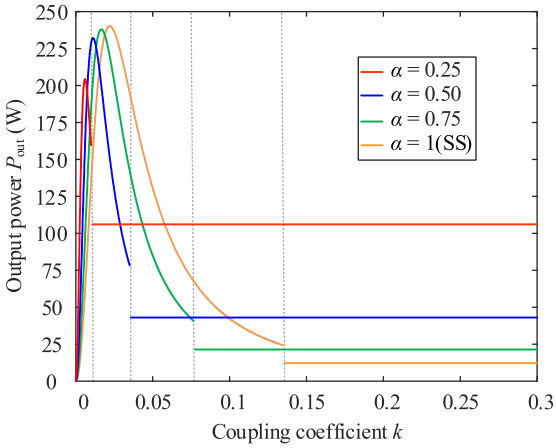

Fig. 7. Curves of output power versus coupling coefficient with different capacitance distribution ratios.

the capacitance distribution ratio. The corresponding curves are shown in Figs. 4 and 5. When the load resistance is much larger than the internal resistance of coil, the system transmission efficiency is significantly improved. But larger load resistance increases the critical coupling coefficient. Therefore, a 20 Ω load resistance is chosen to analyze the system characteristics.

Fig. 6 shows the system frequency bifurcation curves of the WPT system in the exact PT-symmetric region. There are three working frequencies for each coupling coefficient k to ensure the stable operation of the system. Hence, the bifurcation of this system is the triple bifurcation. Different capacitance distribution ratios correspond to different frequency bifurcation curves, which are distinguished by different colors.

The critical coupling coefficient k_C of the system decreases with the reduction of α. The proposed system can provide a wider exact PT-symmetric region and increase the degree of freedom. Therefore, compared with the S/S/S three-coil PT-symmetric system, the proposed system expands the transmission distance greatly by reducing the capacitance distribution ratio α.

The capacitance distribution ratio α not only expands the exact PT-symmetric region but also affects the output power P_{out} and transfer efficiency η. And the corresponding curves are shown in Figs. 7 and 8. The left side of the gray dotted line is the broken PT-symmetric region, and the right side is the exact PT-symmetric region. Although different capacitance distribution ratios lead to different transfer efficiency and output power curves, the output power and transfer efficiency remain constant with the change of the coupling coefficient in the exact PT-symmetric region.

It can be seen from Figs. 7 and 8 that when the input voltage and load resistance are fixed, a smaller α can extend the transmission distance and enhance the output power of the proposed system, but it also reduces the transfer efficiency.

Therefore, we need to design an appropriate value of α based on different application scenarios in practice, and improve the transfer efficiency as much as possible when the output power and transmission distance meet the product requirements. By comparing Figs. 7 and 8, it can be found that the critical coupling coefficient k_C of the WPT system decreases from 0.1350 to 0.0349 when the capacitance distribution ratio $\alpha = 0.5$, which

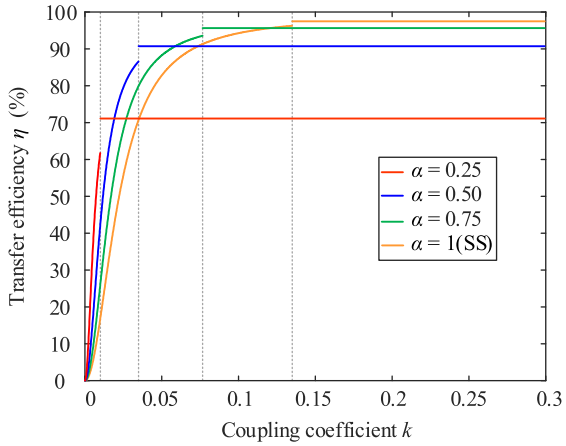

Fig. 8. Curves of transfer efficiency versus coupling coefficient with different capacitance distribution ratios.

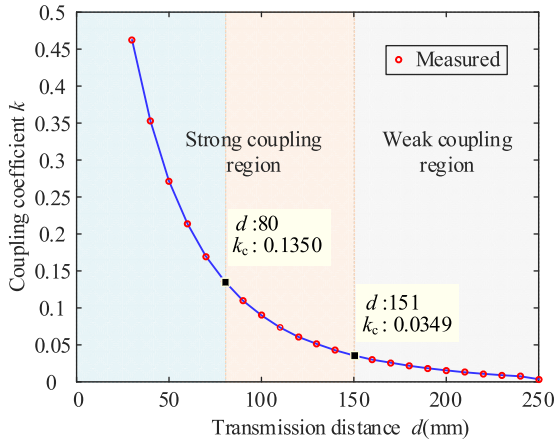

Fig. 10. Measured results of coupling coefficient between adjacent coils versus transmission distance.

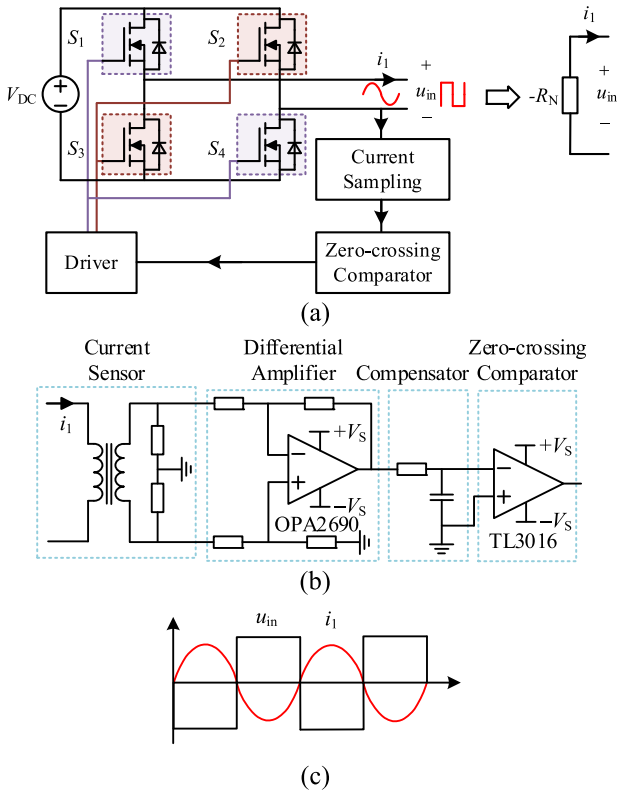

Fig. 9. Schematic of the negative resistance -R_N implementation circuit. (a) Circuit topology. (b) Block diagram of the controller. (c) Steady state voltage and current of -R_N.

extends the transmission distance effectively and maintains a higher output power and transfer efficiency.

III. System Implementation

A. Design of the Negative Resistor

The design of the negative resistor is the most important part of the proposed system, which ensures that the system can achieve PT symmetry. The negative resistor circuit is shown in Fig. 9(a). A self-oscillating controlled full-bridge inverter is used to realize the negative resistor in the article.

The current of the transmitting coil is used as a feedback signal to generate the driving signals of the four switches in the full-bridge inverter. The detailed scheme of controller is shown in Fig. 9(b). First, the current of transmitter is collected by a current sensor (CU8965). Then, an operational amplifier (OPA2690) is used to convert the current single into the voltage single. Finally, the control signals of the full-bridge inverter circuit are generated by the zero-crossing comparator (TL3016). And the control signals of S_1 and S_4, S_2, and S_3 are the same, respectively.

The voltage-current characteristic of the negative resistor is achieved by a zero-crossing comparator, maintaining a 180° phase difference between the output voltage and the current of the full-bridge inverter, as shown in Fig. 9(c). Therefore, the output of the full-bridge inverter can always be equivalent to a negative resistor.

In addition, the fundamental component of the output voltage of the inverter can be derived as

$$U_{\text{in}} = 2\sqrt{2}\frac{V_{\text{dc}}}{\pi}. \tag{22}$$

B. Coupling Coil Design

The planar-spiral coil is easy to manufacture and space-efficient, hence, this structure is suitable for most application scenarios. Accordingly, the transmitting coil, relay coil, and receiving coil in this article are designed as the planar-spiral structure of the same size. Litz wire (Φ0.1 mm×450) is tightly wound to reduce the skin effect. The outer diameter of the coil is 160 mm, and the inner diameter is 115 mm.

The precise impedance analyzer (Wayne Kerr 6500B) is used to measure the coupling coefficient between adjacent coils, as shown in Fig. 10. The blue area is the exact PT-symmetric region of the S/S/S PT-symmetric system. The maximum transmission distance between adjacent coils is 80 mm, and the maximum total transmission distance is 160 mm. The blue and orange parts are the exact PT-symmetric region of the S/S/PS PT-symmetric

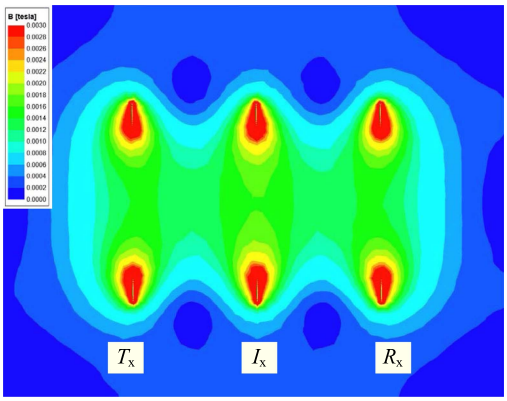

Fig. 11. Magnetic field distribution of the coil structure adopted in the proposed system.

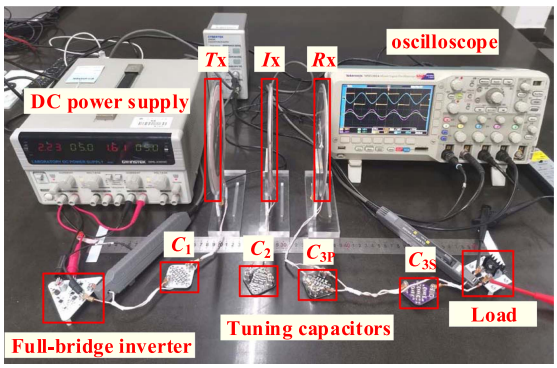

Fig. 12. Experimental platform of the proposed WPT system based on PT symmetry.

WPT system when $\alpha = 0.5$. The maximum transmission distance between adjacent coils is 151 mm, and the maximum total transmission distance is 302 mm. As a result, the transmission distance of the proposed system is approximately twice that of the original three-coil PT-symmetric system.

To analyze the coupling strength among the coils against the transfer distance, the finite element analysis of a three-dimension model using MAXWELL is conducted. Fig. 11 shows the magnetic field distribution when the transmission distance is 200 mm. The coupling coefficient between adjacent coils is 0.09, and the coupling coefficient between nonadjacent coils is only 0.01. The method proposed in this article is dedicated to extending the transmission distance, so the mutual inductance between nonadjacent coils can be ignored in theoretical analysis.

IV. Experimental Verification

In order to validate the proposed theoretical analysis and the parameter design method, the coaxial S/S/PS three-coil WPT system based on the PT-symmetric principle is established as shown in Fig. 12. Dc power supply (GPS-4303C) is used to provide dc input voltage for the whole system. The load of the system is a 20 Ω thick film noninductive power resistor. The design parameters of the proposed three-coil WPT system are shown in Table II.

TABLE II
Parameters of the System

Symbol	Value
L_1	45.58 μH
L_2	45.37 μH
L_2	45.36 μH
C_1	4.018 nF
C_2	4.027 nF
C_{3S}	2.008 nF
C_{3P}	2.008 nF
r_1	0.27 Ω
r_2	0.24 Ω
r_3	0.24 Ω
R_L	20 Ω
f_0	371.7 kHz
V_{dc}	18 V

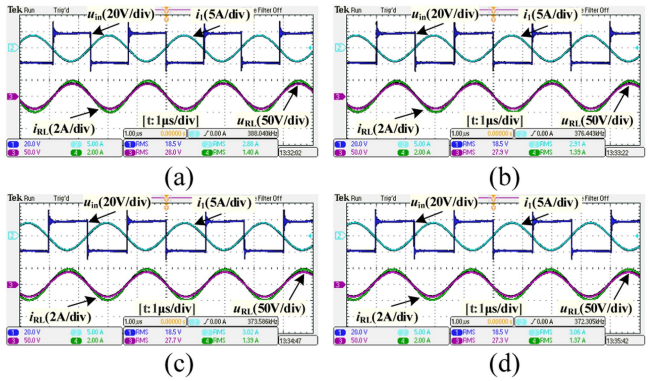

Fig. 13. Experimental waveforms of the receiving coil at different distances. (a) $d = 100$ mm. (b) $d = 180$ mm. (c) $d = 260$ mm. (d) $d = 290$ mm.

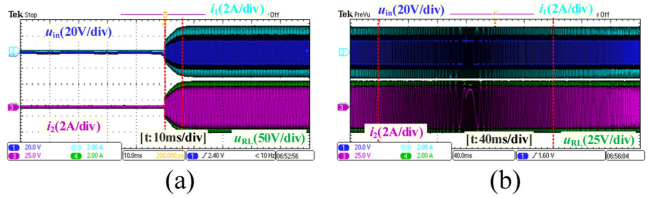

Fig. 14. Dynamic process of the proposed system. (a) Startup state with $d = 100$ mm. (b) Transmission distance from 180–200 mm.

For ensuring that the coupling coefficients between adjacent coils are equal, the transmitting coil T_X, the relay coil I_X, and the receiving coil R_X are placed equidistantly in different positions within the exact PT-symmetric region. The measured experimental waveforms are shown in Fig. 13.

It can be seen from Fig. 13 that even if the relay coil I_X and the receiving coil R_X are at different distances, the phase difference between the input voltage and current is always maintained at 180 °, hence, the proposed method can always maintain the condition of the negative resistor.

Fig. 14(a) shows the start-up waveforms of the system when the transmission distance is 100 mm, and it takes 6 ms to

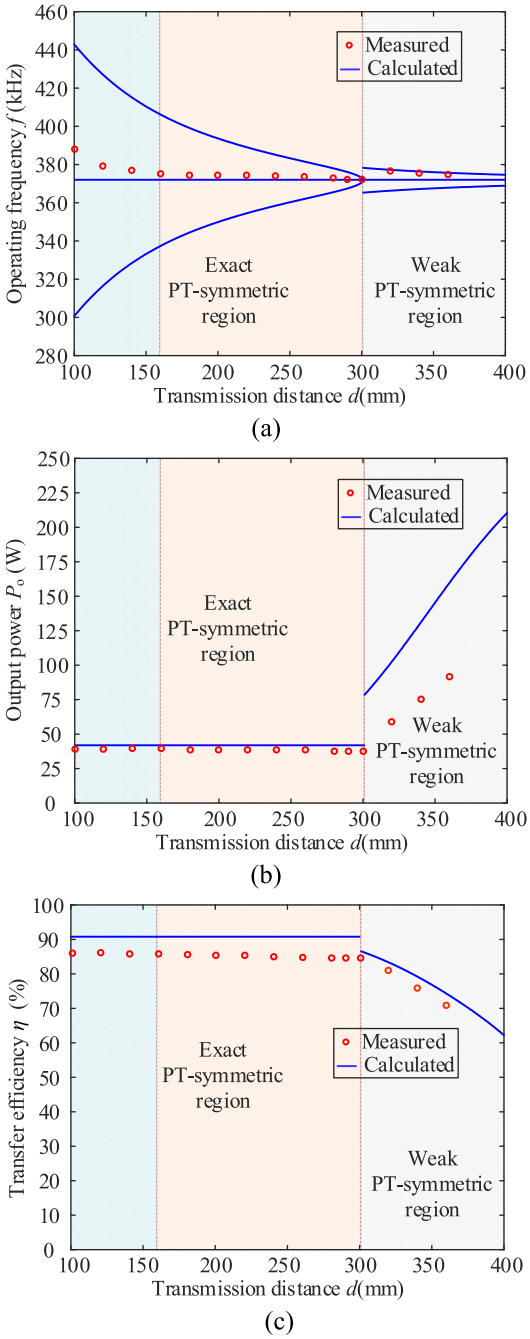

Fig. 15. Transmission characteristics of the three-coil PT-symmetric WPT system when $\alpha = 0.5$. (a) Operating frequency f versus transmission distance d. (b) Output power P_{out} versus transmission distance d. (c) Transfer efficiency η versus transmission distance d.

reach the steady state from start-up. When the coils are rapidly moved from 180–200 mm, the proposed system can quickly reach the steady state, and the dynamic process is shown in Fig. 14(b), which demonstrates that the proposed system has a good dynamic performance in the exact PT-symmetric region.

According to the theoretical analysis in Section II-B, the system automatically operates in the exact PT-symmetric region or resonant state. When $\alpha = 0.5$, the system data of operating frequency f, output power P_{out}, and transfer efficiency η are

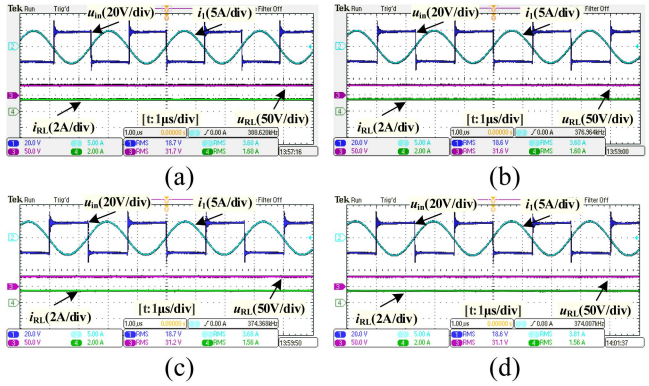

Fig. 16. Experimental waveforms of the receiver with rectifier at different distances. (a) d = 100 mm. (b) d = 180 mm. (c) d = 260 mm. (d) d = 290 mm.

delineated in Fig. 15. The blue curves are the theoretical data, and the red circles are the experimental measured data.

When the transmission distance $d < 300$ mm, the system is in the exact PT-symmetric region. The blue area is the exact PT-symmetric region of the traditional PT-symmetric system. And the orange area is the extended exact PT-symmetric region by the proposed system with $\alpha = 0.5$. The exact PT-symmetric region is almost doubled. In Fig. 15(a), the operating frequencies of the system highly meet the vicinity of the natural resonance frequency. As seen from Fig. 15(b) and (c), the transfer efficiency of the system maintains at about 85%, while the output power is constant near 38 W.

The system operates in the broken PT-symmetric region when the transmission distance $d > 300$ mm. The transfer efficiency and output power of the system vary with the transmission distance. For the stable operation of the WPT system, the system should be avoided to work in the broken PT-symmetric region.

In order to verify the practicability of the method proposed in this article, the diode rectifier with a filter capacitor is added at the receiving side. When the relay coil and the receiving coil move coaxially and equidistantly in the exact PT-symmetric region, the measured experimental waveforms are shown in Fig. 16. From the experimental data, it can be seen that the output voltage is constant near 31 V. Therefore, the output power remains constant 48 W regardless of the transmission distance.

There are certain errors between the experimental data and the theoretical data. First, we equalize the SP compensation network as the S compensation network and ignore the small mutual inductance between nonadjacent coils to simplify the theoretical analysis. When the transmission distance of the system is relatively short, the coupling coefficient between nonadjacent coils becomes large and affects the system operating frequency, but the proposed system can still maintain PT symmetry. Second, the internal resistance of the relay coil is ignored in the theoretical analysis in order to make the three-coil S/S/PS compensation network WPT system satisfy the PT symmetry. However, the internal resistance of the coupling coil can only be controlled as small as possible in reality. What is more, the internal resistance loss of the coil has a greater impact on the system when the transmission distance is longer. Finally, the measurement equipment will also cause errors in the experimental results.

The experimental results and the theoretical calculation have similar trends in different transmission distances, and the errors are within the permission in the exact PT-symmetric region. Therefore, the experimental results verify that the S/S/PS compensation network can significantly improve the transmission distance and output power of the three-coil PT-symmetric WPT system.

V. Conclusion

In order to further improve the transmission distance and output power of the PT-based WPT system, a novel S/S/PS compensation network three-coil WPT system based on the PT-symmetric principle has been proposed. The parallel capacitor of the receiving coil increases the complexity of the system modeling. Hence, the high-order PS compensation network is first equivalent to the low-order S compensation network by using the equivalent circuit method. Then, the mathematical model of the proposed system is established by the CMT. The expressions of the operating frequency, output power, and transfer efficiency of the proposed system are obtained. Compared with the traditional S/S/S PT-symmetric system, the proposed system extends the transmission distance and improves the output power significantly with the same input voltage and load resistance. Furthermore, the proposed system can adapt to more application scenarios by designing the capacitance distribution ratio α. The experimental results demonstrate that the exact PT-symmetric region of the proposed system is nearly twice that of the original three-coil PT-symmetric system when $\alpha = 0.5$, while maintaining the constant output power of about 48 W and the transfer efficiency of about 85%.

References

[1] M. Kim, D. -M. Joo, and B. K. Lee, "Design and control of inductive power transfer system for electric vehicles considering wide variation of output voltage and coupling coefficient," *IEEE Trans. Power Electron.*, vol. 34, no. 2, pp. 1197–1208, Feb. 2019.

[2] A. Zakerian, S. Vaez-Zadeh, and A. Babaki, "A dynamic WPT system with high efficiency and high power factor for electric vehicles," *IEEE Trans. Power Electron.*, vol. 35, no. 7, pp. 6732–6740, Jul. 2020.

[3] M. R. Basar, M. Y. Ahmad, J. Cho, and F. Ibrahim, "Stable and high-efficiency wireless power transfer system for robotic capsule using a modified helmholtz coil," *IEEE Trans. Ind. Electron.*, vol. 64, no. 2, pp. 1113–1122, Feb. 2017.

[4] J. -Q. Zhu, Y. -L. Ban, Y. Zhang, Z. Yan, R. -M. Xu, and C. C. Mi, "Three-Coil wireless charging system for metal-cover smartphone applications," *IEEE Trans. Power Electron.*, vol. 35, no. 5, pp. 4847–4858, May 2020.

[5] H. Li, J. Fang, S. Chen, K. Wang, and Y. Tang, "Pulse density modulation for maximum efficiency point tracking of wireless power transfer systems," *IEEE Trans. Power Electron.*, vol. 33, no. 6, pp. 5492–5501, Jun. 2018.

[6] H. Feng, T. Cai, S. Duan, J. Zhao, X. Zhang, and C. Chen, "An LCC-Compensated resonant converter optimized for robust reaction to large coupling variation in dynamic wireless power transfer," *IEEE Trans. Ind. Electron.*, vol. 63, no. 10, pp. 6591–6601, Oct. 2016.

[7] S. Y. R. Hui, W. Zhong, and C. K. Lee, "A critical review of recent progress in mid-range wireless power transfer," *IEEE Trans. Power Electron.*, vol. 29, no. 9, pp. 4500–4511, Sep. 2014.

[8] D. Ahn and S. Hong, "Wireless power transmission with self-regulated output voltage for biomedical implant," *IEEE Trans. Ind. Electron.*, vol. 61, no. 5, pp. 2225–2235, May 2014.

[9] J. P. Chow, H. S. Chung, and C. Cheng, "Use of transmitter-side electrical information to estimate mutual inductance and regulate receiver-side power in wireless inductive link," *IEEE Trans. Power Electron.*, vol. 31, no. 9, pp. 6079–6091, Sep. 2016.

[10] D. W. Seo and J. H. Lee, "Frequency-tuning method using the reflection coefficient in a wireless power transfer system," *IEEE Microw. Wireless Compon. Lett.*, vol. 27, no. 11, pp. 959–961, Nov. 2017.

[11] L. Chen, S. Liu, Y. C. Zhou, and T. J. Cui, "An optimizable circuit structure for high-efficiency wireless power transfer," *IEEE Trans. Ind. Electron.*, vol. 60, no. 1, pp. 339–349, Jan. 2013.

[12] Y. Lim, H. Tang, S. Lim, and J. Park, "An adaptive impedance-matching network based on a novel capacitor matrix for wireless power transfer," *IEEE Trans. Power Electron.*, vol. 29, no. 8, pp. 4403–4413, Aug. 2014.

[13] J. Kim, D. Kim, and Y. Park, "Analysis of capacitive impedance matching networks for simultaneous wireless power transfer to multiple devices," *IEEE Trans. Ind. Electron.*, vol. 62, no. 5, pp. 2807–2813, May 2015.

[14] W. X. Zhong and S. Y. R. Hui, "Maximum energy efficiency tracking for wireless power transfer systems," *IEEE Trans. Power Electron.*, vol. 30, no. 7, pp. 4025–4034, Jul. 2015.

[15] X. Tang, J. Zeng, K. P. Pun, S. Mai, C. Zhang, and Z. Wang, "Low-Cost maximum efficiency tracking method for wireless power transfer systems," *IEEE Trans. Power Electron.*, vol. 33, no. 6, pp. 5317–5329, Jun. 2018.

[16] Z. Yan et al., "Efficiency improvement of wireless power transfer based on multitransmitter system," *IEEE Trans. Power Electron.*, vol. 35, no. 9, pp. 9011–9023, Sep. 2020.

[17] C. M. Bender and S. Boettcher, "Real spectra in non-Hermitian Hamiltonians having PT symmetry," *Phys. Rev. Lett.*, vol. 80, 1998, Art. no. 5243.

[18] V. B. Braginsky and S. P. Vyatchanin, "Low quantum noise tranquilizer for Fabry-Perot interferometer," *Phys. Lett. A*, vol. 293, pp. 228–234, 2002.

[19] T. J. Kippenberg and K. J. Vahala, "Cavity optomechanics: Back-action at the mesoscale," *Science*, vol. 321, pp. 1172–1176, 2008.

[20] S. Assawaworrarit, X. Yu, and S. Fan, "Robust wireless power transfer using a nonlinear parity–time-symmetric circuit," *Nature*, vol. 546, no. 7658, pp. 387–390, Jun. 2017.

[21] J. Zhou, B. Zhang, W. Xiao, D. Qiu, and Y. Chen, "Nonlinear parity-time-symmetric model for constant efficiency wireless power transfer: Application to a Drone-in-Flight wireless charging platform," *IEEE Tran. Ind. Electron.*, vol. 66, no. 5, pp. 4097–4107, May 2019.

[22] L. Wu, B. Zhang, and J. Zhou, "Efficiency improvement of the parity-time-symmetric wireless power transfer system for electric vehicle charging," *IEEE Tran. Power Electron.*, vol. 35, no. 11, pp. 12497–12508, Nov. 2020.

[23] L. Yang, X. Li, S. Liu, Z. Xu, C. Cai, and P. Guo, "Analysis and design of three-coil structure WPT system with constant output current and voltage for battery charging applications," *IEEE Access*, vol. 7, pp. 87334–87344, Jun. 2019.

[24] X. Liu, X. Song, and X. Yuan, "Compensation optimization of the relay coil in a strong coupled coaxial three-coil wireless power transfer system," *IEEE Trans. Power Electron.*, vol. 37, no. 4, pp. 4890–4902, Apr. 2022.

[25] X. Shu, B. Zhang, Z. Wei, C. Rong, and S. Sun, "Extended-Distance wireless power transfer system with constant output power and transfer efficiency based on parity-time-symmetric principle," *IEEE Trans. Power Electron.*, vol. 36, no. 8, pp. 8861–8871, Aug. 2021.

[26] C. Rong, B. Zhang, Z. Wei, L. Wu, and X. Shu, "A wireless power transfer system for spinal cord stimulation based on generalized parity–time symmetry condition," *IEEE Trans. Ind. Appl.*, vol. 58, no. 1, pp. 1330–1339, Jan./Feb. 2022.

[27] M. Kiani and M. Ghovanloo, "The circuit theory behind coupled-mode magnetic resonance-based wireless power transmission," *IEEE Trans. Circuits Syst. I, Reg. Papers*, vol. 59, no. 9, pp. 2065–2074, Sep. 2012.

Yuhu Qu was born in Shanxi, China, in 1998. He received the B.S. degree in electrical engineering from the School of Mechatronic Engineering and Autonation, Shang Hai University, Shanghai, China, in2020. He is currently working toward the M.S. degree in energy dynamics with the School of Electric Power, South China University of Technology, Guangzhou, China.

His current research interests include wireless power transfer applications and power electronics.

Bo Zhang (Senior Member, IEEE) was born in Shanghai, China, in 1962. He received the B.S. degree in electrical engineering from Zhejiang University, Hangzhou, China, in 1982, the M.S. degree in power electronics from Southwest Jiaotong University, Chengdu, China, in 1988, and the Ph.D. degree in power electronics from the Nanjing University of Aeronautics and Astronautics, Nanjing, China, in 1994.

He is currently a Professor with the School of Electric Power, South China University of Technology, Guangzhou, China. He has authored or coauthored six books in IEEE–Wiley and Springer and more than 500 technical papers, and he holds 130 patents. His current research interests include nonlinear analysis, modeling and control of power electronic converters, and wireless power transfer applications.

Wenchao Gu was born in Jiangxi, China, in 1998. He received the B.S. degree in automation from Nanchang University, Nanchang, China, in 2020. He is currently working toward the M.S. degree in power electronics with the School of Electric Power, South China University of Technology, Guangzhou, China.

His research interests include wireless power transfer applications and power electronic converters.

Xujian Shu received the B.S. degree in electrical engineering and automation from China University of Mining and Technology, Xuzhou, China, in 2015, and the Ph.D. degree in power electronics from South China University of Technology, Guangzhou, China, in 2021.

She is currently with Fuzhou University, Fuzhou, China. Her research interests include wireless power transfer applications, power electronics converters, and fractional-order system.